

# Mould flux crystallization: A kinetic study

R. CARLI and C. RIGHI  
*Prosimet SpA, Filago BG Italy*

In modern steel continuous casting technologies mould fluxes are well-known to assure lubrication required by tribological system of mould-solidifying strand shell, and to provide crystalline phase solid film, contributing to control heat extraction between strand and mould wall.

Actual cooling rates during normal continuous casting operations are far higher than critical cooling rate of the liquid slag. Indeed, DTA measurements point out that even relatively small cooling rates of 30–50 K/min are high enough to give exiguous formation of crystals.

In this paper, contribution of devitrification in defining crystalline phase formation of industrial basic mould slag, used in continuous casting of crack-sensitive steel grades, has been investigated by means of non-isothermal experiments study.

Devitrification has proved to play a major role in mould flux crystallization in a working environment explaining the higher amount of crystalline phase formed in plant sample in comparison with lab sample from DTA analysis with typical cooling rate of 5–20 K/min. The amount of crystalline phases formed ranks as follow: Cuspidine > Combeite > Gehlenite.

Kinetic analysis of DTA non-isothermal experiments has provided kinetic parameters through Kissinger and Ozawa methods, as Avrami constant resulting to be  $n \cong 2$  and activation energy of Cuspidine crystallization resulting to be  $E_C = 315$  kJ/mole.

The effect of addition to the parent material of oxides as MnO, TiO<sub>2</sub>, ZrO<sub>2</sub>, Al<sub>2</sub>O<sub>3</sub> and Fe<sub>2</sub>O<sub>3</sub> near to saturation point has proved to affect, in certain cases, crystallization behaviour of mold flux. In particular, MnO, TiO<sub>2</sub>, ZrO<sub>2</sub> oxides produce a relevant dump of crystallization of Combeite and Gehlenite phases, while Al<sub>2</sub>O<sub>3</sub> and Fe<sub>2</sub>O<sub>3</sub> do not appreciably affect crystallization.

Key words: Mould flux, crystallization, devitrification, DTA non-isothermal analysis, Kissinger and Ozawa methods.

## Introduction

In modern steel continuous casting technologies mold fluxes are well-known to assure lubrication required by tribological system of mold/solidifying strand shell and to provide crystalline phase solid film contributing to control heat extraction between strand and mold wall. The study of formation of crystalline phases in thin mould flux layer is of considerable practical interest.

Common methods applied to the study of crystallization behaviour of mould fluxes range within a wide number of techniques. The most accurate approach in studying such phenomenon has proved to be construction of isothermal time temperature transformation diagrams (TTT curves) or continuous cooling transformation diagrams (CCT curves)<sup>1-2</sup>. To avoid uncertainties due to estimation of crystalline phase volume, based on direct inspection of solidified slag sample through optical microscopy, it is preferable to measure crystallization heat through DTA or DSC in isothermal and/or non-isothermal experiments. In previous works construction of a section of CCT curves with DTA measurements for mould flux slag samples has been discussed<sup>3-5</sup>.

However, samples of industrial basic slag obtained directly from the shop floor on steel plants show crystalline phase content to be of a larger amount compared to a lab sample obtained from mould flux slag molten at 1573 K and cooled down at a cooling rate of 5–30 K/min. (typical of DTA-DSC experiments). A method developed at Imperial

College, London, UK<sup>6</sup>, based on mould flux slag sample quenching from 1573 K to 773 K and subsequent annealing for 10 minutes at 773 K, shows that the amount of crystalline phase formed is comparable to actual case of plant sample. This method tries to represent, more accurately, actual cooling conditions in working environment where cooling rates during normal continuous casting mould operations are far higher than the critical cooling rate of the liquid slag.

Results obtained by this method suggest that devitrification plays a major role in defining crystalline phase formation of mould slag in working environment. Therefore, in present study, devitrification of industrial basic mould slag sample, used in continuous casting of crack-sensitive steel grades, has been investigated by means of DTA non-isothermal experiments. Kinetic analysis of such non-isothermal experiments provided kinetic parameters through Kissinger and Ozawa methods. Further XRD and SEM characterizations give a fairly exhaustive understanding of complex crystallization behaviour of mould flux sample under study.

## Experimental

### Materials

Experiments were carried out on lab samples in loose powder form named parent material (MM) and doped

material (BX) respectively, BM (MnO doping), BT (TiO<sub>2</sub> doping), BZ (ZrO<sub>2</sub> doping), BA (Al<sub>2</sub>O<sub>3</sub> doping) and BF (Fe<sub>2</sub>O<sub>3</sub>) doping.

Parent material was prepared using standard raw materials analysed and certified by Prosimet laboratory. Doped materials were prepared starting from parent material by addition of weighed quantities of following pure compounds: MnO (II) from Aldrich Chemical Co. (99.99 + per cent); TiO<sub>2</sub> (IV) from Fluka Chemie AG (99.99 per cent); ZrO<sub>2</sub> (IV) from Aldrich Chemical Co. (99.99 per cent); Al<sub>2</sub>O<sub>3</sub> NO. 102 Nabalox at 99.5 per cent from Nabaltec GmbH; Fe<sub>2</sub>O<sub>3</sub> (III) from Aldrich Chemical Co. (99.99 per cent).

### Experimental apparatuses

Raw materials and pure chemical compounds were mechanically mixed by powder lab blender IG/MS by Giuliani Tecnologie Srl (Italy).

Sampling of materials under study was performed by means of a rotating divider PK 1000 equipped with a vibratory feeder DR 100/75 by Retsch GmbH (Germany): this instrumentation procured a representative and homogeneous sample of powder of fixed amount (e.g. 20 g) starting from a bigger sample (e.g. 100 g) avoiding errors due to mass effect.

Heating treatment of samples at 923 K and at 1573 K was performed in the same furnace respectively in an Inconel (Ni-Cr-Fe alloy 601) crucible from Sigma-Aldrich Chemical Co. and in a platinum gold crucible (alloy at 5 per cent in gold) from Metalli Preziosi SpA, Italy, (Johnson Matthey Group).

Quenching apparatus was constituted by a home designed couple of copper discs 40 mm in height and 150 mm in width (in diameter).

Milling of glassy samples produced during, melting process was performed by rotating mill HSM 100H by Herzog GmbH equipped with stainless steel grinding system.

Chemical characterization was realized by carbon-sulphur IR determinator CS 200 by Leco Co. (U.S.A) (analytical software CS 200 Version 1.21) and by PW 2400 XRF Sequential Spectrometer with VCR-2540 sample changer equipment by PANalytical - former Philips - (analytical software SuperQ Version 2.0C).

Differential Thermal Analysis measurements were carried out by means of L62 DTA instrument, equipped with controller L70/215C and data acquisition card L70/2001 from Linseis GmbH (Germany). This apparatus was modified by installing a Pt-Rh sample holder for better quantitative evaluation of heat changes. Data elaboration was provided by software WIN-HDSC by Linseis.

XRD instrumentation was diffractometer D-8000 from Brüker, equipped with a home designed hot chamber able to reach maximum heating temperature of 1773 K.

Electronic microscopy apparatus was PANalytical XL 30 ESEM-FEG (environmental scanning electronic microscope with field emission gun, at low vacuum) equipped with hot chamber with maximum working temperature of 1273 K.

### Experimental procedures

#### Samples preparation and characterization

Parent material was prepared by mechanically mixing in the lab blender for half an hour of the different standard industrial raw materials obtaining 1000 g of product named MM.

By means of a rotating sample divider six 100 g samples of MM product were obtained, the first one being reference sample of MM material, the other five representing bases to prepare doped materials.

Doped materials BM, BT, BZ, BA and BF were prepared in the same lab mixer with a mixing time of 15 minutes starting from weighed quantities of parent material MM (about 95 g, depending on the final content of doping oxide) and related pure chemical compound.

Suitable amount of all these samples were characterized consistently with standard C, S content determination and XRF analytical procedures in order to ascertain correspondence to fixed formulations.

In Table I chemical analyses related to parent and doped materials expressed in weight percentage (normalized to 100 per cent without expressing loss on ignition) are reported: referring to quenched slag chemical analyses losses in fluorine content have not been accounted for.

#### Quenched slag preparation

All samples were heated at 923 K for 12 hours in furnace in Inconel crucible to make carbon burn off allowing, also, the carbonates to decompose. This pre-treatment of samples was performed in order to facilitate successive melting of samples.

Once sintered samples were cooled to room temperature, simply extracting them from furnace, they were recovered from the crucible and milled for 30 s in the Herzog rotating mill to be in the suitable physical condition required by successive sampling operations.

Consequently a sampling was performed by use of a rotating divider in order to get 20 g of material for each sample.

This amount of powder was placed in the Pt-Au crucible in the furnace at 1573 K for 7 minutes which represents the minimum period of time necessary to the complete melting of material.

Molten slags at 1573 K were extracted from furnace and rapidly poured on to the first copper disc and immediately squeezed with the other one. In this way a fast quenching, to room temperature, of molten slag was realized.

A few minutes after, it was possible to find a layer of glassy material divided into small pieces with a thickness of about 1 mm.

These various fragments of glassy material having different sizes (from 1–2 mm to 40 mm) were recovered and milled for 60 s by a grinding system getting fine powder with average dimensions of particle under 100 µm.

**Table I**  
Chemical analyses of parent and doped materials expressed in weight percentage

	MM	BM	BT	BZ	BA	BF
SiO <sub>2</sub>	39.1	36.6	37.1	38.0	38.6	37.1
Fe <sub>2</sub> O <sub>3</sub>	0.5	1.0	0.5	0.5	0.5	5.8
Al <sub>2</sub> O <sub>3</sub>	2.5	2.7	2.7	2.7	4.7	2.7
CaO	44.4	41.3	41.9	42.8	43.6	41.8
MgO	1.3	1.2	1.2	1.2	1.2	1.2
Na <sub>2</sub> O	6.5	6.1	6.1	6.1	6.1	6.1
F-	5.6	5.2	5.2	5.2	5.2	5.2
MnO	0	5.9	0	0	0	0
TiO <sub>2</sub>	0	0	5.3	0	0	0
ZrO <sub>2</sub>	0	0	0	3.5	0	0

Samples in the form of fine powder named respectively GMM, GBM, GBT, GBZ, GBA and GBF adding a G as a prefix to original denominations were so prepared for XRD, ESEM and DTA analyses.

### DTA analytical procedure

Analytical procedure was as follows a for each sample analyzed: two Pt-Rh crucibles filled with about 70 mg of Al<sub>2</sub>O<sub>3</sub> NO. 102 Nabalox at 99.5 per cent from Nabaltec GmbH as reference material and 70 mg of glassy samples reduced to fine powder were allocated in defined positions on to the stage holder.

Crucibles were heated from RT to 1623 K at different heating rates (5, 10, 15, 20, 25 K per minute).

## Results and discussions

### DTA and SEM analyses on GMM sample

DTA experiments were conducted as described in previous paragraph at heating rate of 20 K/min on glassy sample GMM. DTA measurements on our samples pointed out complex nature of devitrification of these materials.

In Figure 1, exothermic peaks appearing for crystallization of glassy sample GMM suggest the presence of different phases. Two well-defined peaks P<sup>I</sup> and P<sup>II</sup>, showing T<sub>C</sub> of 952 K and 1073 K, support consecutive crystallization of at least two phases. Further XRD investigations of the same material carried out with Brüker D-8000 diffractometer equipped with hot chamber, allowing heating of sample at stepping rate of 2 K/min showed crystallization kinetics of three phases, namely Cuspidine (T<sub>C</sub> ≅ 973 K), Combeite (TC ≅ 1023 K) and Gehlenite (T<sub>C</sub> 1073 K), see Figure 2.

It can be concluded that P<sup>I</sup> corresponds to crystallization of Cuspidine phase, while P<sup>II</sup> comes from convolution of two peaks related to crystallization of Combeite and Gehlenite phases.

The amount of crystalline phase formation has been evaluated through Prosimet Crystallization Index, PCIn, which is a percentage of a reference crystallization peak area,  $\tilde{P}_A = 34.2 (\mu V \cdot s/mg) \equiv 100 \%$ .

Comparison of peaks area (P<sup>I</sup> + P<sup>II</sup>) obtained for devitrification, (PCIn)<sub>DH</sub> ~ 99.9 %, and peaks area of crystallization obtained in DTA cooling of molten MM sample (T<sub>0</sub> = 1673 K, cooling rate 20 K/min.), (PCIn)<sub>CC</sub> ~ 51.0 %<sup>3</sup>, indicates that devitrification is quantitatively much more relevant phenomenon, as far as total amount of crystalline phase actually formed, is concerned.

Another interesting phenomenon was observed in an experiment carried out with PANAnalytical ESEM microscope. *In situ* heating GMM sample with high temperature hot stage at 50 K/min under dry air atmosphere (2 Torr) revealed that as a consequence of devitrification sample surface went progressively more and more corrugated, see Figure 3 A and B.

Based on these observations some conclusions can be drawn.

- Devitrification quantitatively explain higher amount of crystalline phase observed for plant sample of slag film than for lab sample cooled at 10÷30 K/min (typical DTA cooling rates)
- Crystalline phases observed have been effectively related to peaks measured in DTA experiments due to remarkable consistency of T<sub>C</sub> from DTA and XRD measurements. Amount of crystalline phases formed ranks as follow: Cuspidine > Combeite > Gehlenite
- Devitrification actually contributes to radiative part of effective conductivity (crystalline phase formation) and contact resistance at the mould/slag interface (more corrugated surface)<sup>7-8</sup>.

### Cuspidine crystallization kinetic

Unequivocal characterization of crystalline phase corresponding to DTA measured peak, P<sup>I</sup>, allows consistent

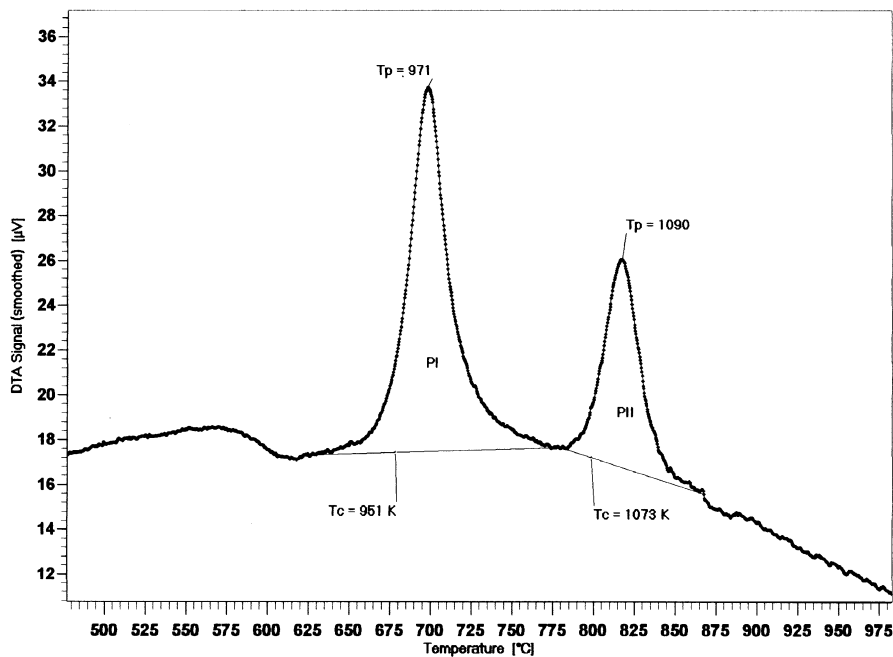


Figure 1. DTA of GMM sample

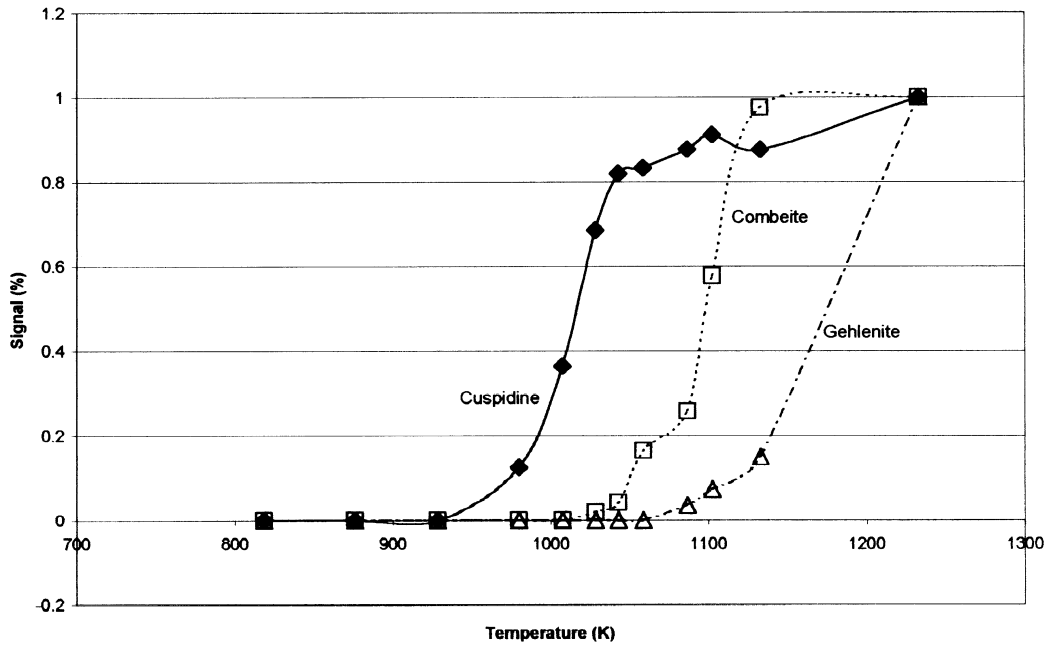
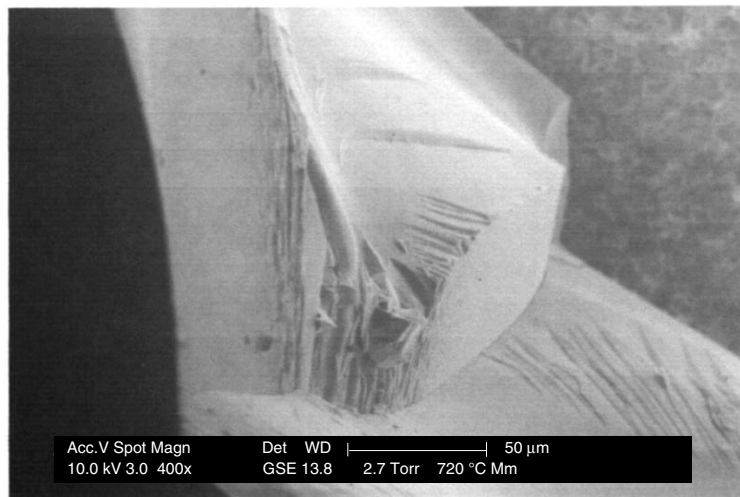


Figure 2. Amount of crystalline phases formed against temperature, XRD measurements

A



B

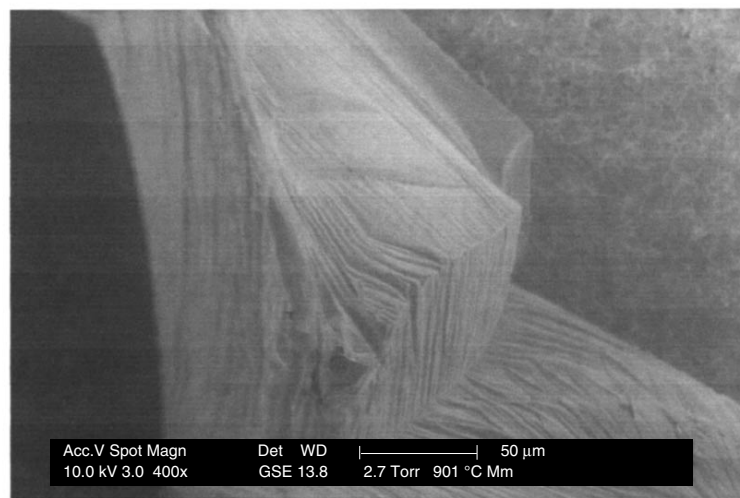


Figure 3. A) ESEM image of GMM sample heated at 993 K; B) ESEM image of same sample heated at 1174 K

study of Cuspidine crystallization kinetic. Indeed, variation of crystallization peaks with different DTA heating rates can be used to estimate the activation energy of crystallization (Arrhenius law) and to determine crystallization mechanism. Therefore, several experiments were carried out on devitrification of GMM samples at different heating rates.

Ozawa equation<sup>9</sup> allows determination of Avrami constant,  $n$ , resulting to be  $n \cong 2$ . This is consistent with sharpness of measured peak, suggesting bulk crystallization process to be responsible for Cuspidine crystallization in our samples<sup>9</sup>. Activation energy of crystallization,  $E_C$ , can be determined by classical Kissinger method<sup>10</sup>, resulting  $E_C = 315$  kJ/mole. However, when nucleation takes place during heating, value of  $E_C$  estimated by classical Kissinger method has a considerably lower value compared with value of activation energy of crystal growth,  $E_G$ .

Using modified Kissinger method, as described by Matusita *et al.*<sup>11-13</sup>, and taking into account that Avrami constant has been found to be  $n \cong 2$ , activation energies of crystal growth have been estimated in case of nucleation dependent and independent from heating temperature, resulting to be respectively:  $[E_G]_T = 647$  kJ/mole and:  $[E_G]_{nT} = 323$  kJ/mole. As expected<sup>14</sup>, and consistent with error associated to methods, it results that  $E_G \approx (n/m)E_C$ , where  $m$  stands for dimensionality of crystal growth parameter in Kissinger modified method.

### Effects of doping compounds

The effect of MnO addition, as can be clearly inferred in Figure 4, can be resumed in a sort of dumping of Combeite-Gehlenite phases.

This experimental result is consistent with our previous observations on crystallization behaviour of MnO-doped slags whose CCT (Continuous Cooling Transformation) curves were found to be affected by this compound

addition, resulting in a sharp decrease of DTA temperature of crystallization<sup>3-5</sup>.

Similar effects of dumping were observed in cases of zirconia and titania doping GBZ and GBT, the latter to a greater extent. On the other hand, devitrification patterns in cases of alumina and iron (III) oxide doping for GBA and GBF, were found to be very similar with that of parent material GMM.

The major result is that in all sample P<sup>I</sup>, corresponding to Cuspidine crystallization remains approximately unchanged, see Table II.

### Conclusions

It has been shown that devitrification plays a major role in defining crystalline phase formation of mould slag in working environment. In particular, devitrification quantitatively explain a higher amount of crystalline phase observed for plant sample of slag film than for lab sample cooled at 10÷30 K/min (typical DTA cooling rates). Devitrification actually contributes to radiative part of effective conductivity (crystalline phase formation) and contact resistance at the mould/slag interface (more corrugated surface). Crystalline phases observed have been

**Table II**  
T<sub>C</sub> and T<sub>P</sub> obtained from DTA measurements on all samples

	P <sup>I</sup> T <sub>C</sub>	P <sup>I</sup> T <sub>P</sub>	P <sup>II</sup> T <sub>C</sub>	P <sup>II</sup> T <sub>P</sub>
GMM	952	971	1073	1090
GBM	951	969	-	-
GBT	970	993	-	-
GBZ	970	993	-	-
GBA	982	1005	1135	1151
GBF	965	983	1093	1107

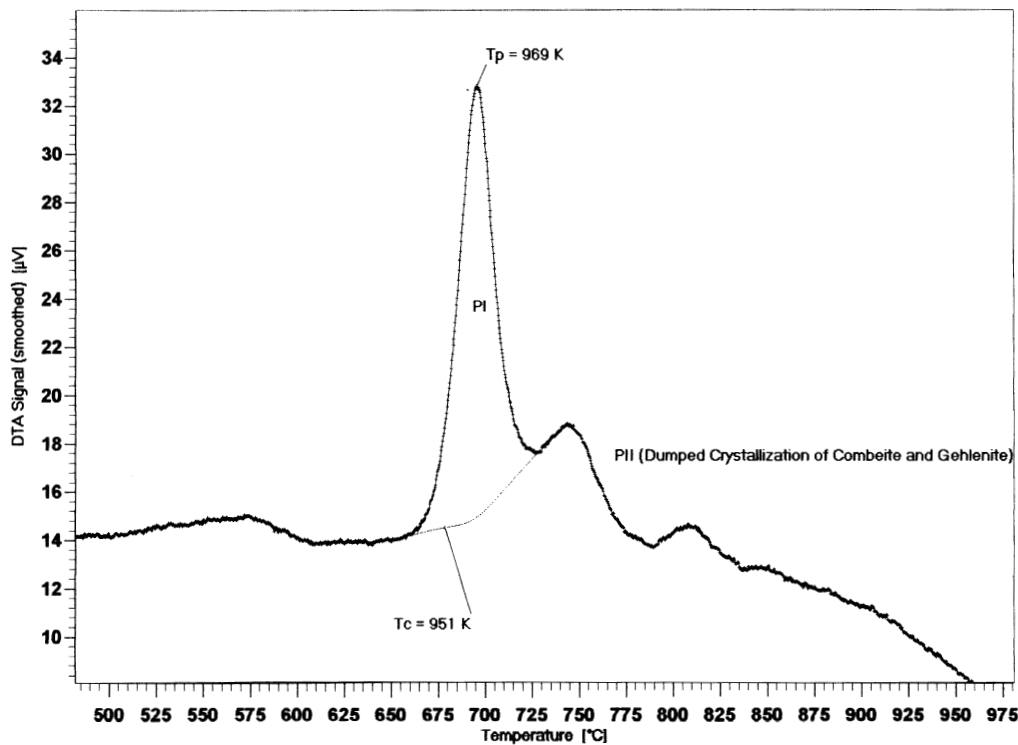


Figure 4. DTA of GBM sample.

effectively related to peaks measured in DTA experiments due to remarkable consistency of  $T_C$  from DTA and hot chamber XRD measurements. Amount of crystalline phases formed ranks as follow: Cuspidine > Combeite > Gehlenite. Bulk crystallization process has proved to be responsible for Cuspidine crystallization in our samples, being Avrami constant from Ozawa equation estimate to be  $n \cong 2$ . Kissinger method provided estimation of activation energy of Cuspidine crystallization, resulting  $E_C = 315$  kJ/mole.

### Acknowledgements

We greatly thank Professor of Mineralogy and Crystallography, Gilberto Artioli of University of Milan, Earth Sciences Department for helpful discussions on subjects and for high temperature XRD measurements, carried out in Diffraction Laboratory by his research assistant Dr. Monica Dapiaggi.

We would like also to thank Mr. Mario Mangiagalli of FEI-PANalytical Company for ESEM measurements at high temperature.

### References

1. KASHIWAYA, Y., CICUTTI, C.E., and CRAMB, A.W. *ISIJ International*, vol. 38, no.4 1998, pp. 357–365
2. ORRLING, C., KASHIWAYA, Y., SRIDHAR, S., and CRAMB, A.W. 'In situ observations and thermal analysis of Crystallization phenomenon in mold slags.' *Proceedings 6th International Conference on Molten Slags Fluxes and Salts*, Stockholm-Helsinki, 2000, CD-ROM file no. 096.
3. CARLI, R. and GHILARDI, V. *Iron & Steelmaker*, vol.25, no.6. 1998. pp. 43–46
4. GHILARDI, V., CARLI, R., and FARAVELLI, G.L. 'Improving technological properties of mold fluxes used in crack sensitive steel grades casting.' *Proceedings 3rd European Conference on Continuous Casting*, Madrid, 1998 pp. 977-980.
5. RIGHI, C., CARLI, R., and GHILARDI, V. 'Any chance of controlling crystallization behaviour of mold fluxes?. New insights?.' *Proceedings 6th International Conference on Molten Slags Fluxes and Salts*, Stockholm-Helsinki, 2000, CD-ROM file no. 102.
6. MILLS, K.C. and LI, Z. private communications, Dept. of Materials, Imperial College, April 2003, London.
7. HOLZHAUSER, J.-F., SPITZER, K.-H., and SCHWERDTFEGER, K. *Steel research* vol. 70, no. 10, 1999, pp.430–436.
8. HOLZHAUSER, J.-F., SPITZER, K.-H., and SCHWERDTFEGER, K. *Steel research* vol. 70, no. 07, 1999, pp. 252–258.
9. OZAWA, T. *Polymer*, vol. 12, 1971, pp. 150–158.
10. KISSINGER, H.E. *Anal. Chem.*, vol. 29, 1957, p. 1702.
11. MATUSITA, K., SAKKA, S., and MATSUI, Y. *J. Mater. Sci.*, vol. 10, pp. 961–966.
12. MATUSITA, K. and SAKKA, S. *J. Non- Cryst. Sol.*, vol. 38–39, 1980, pp. 741–746.
13. MATUSITA, K. and SAKKA, S. *Bull. Inst., Chem. Res. Kyoto Univ.*, vol. 59, 1981, p. 159.
14. XU, X., RAY, C., and DAY, D. *J. Am. Ceram. Soc.* vol. 74 1991, p. 909.